

# Evaluation and Quantitative Attribution Analysis of Water Yield Services in the Peak-cluster Depression Basins in Southwest of Guangxi, China

WANG Donghua<sup>1, 2</sup>, TIAN Yichao<sup>1, 2, 3</sup>, ZHANG Yali<sup>1</sup>, HUANG Liangliang<sup>2</sup>, TAO Jin<sup>1</sup>, YANG Yongwei<sup>1</sup>, LIN Junliang<sup>1</sup>, ZHANG Qiang<sup>1</sup>

(1. School of Resources and Environment, Beibu Gulf University, Qinzhou 535011, China; 2. College of Environmental Science and Engineering, Guilin University of Technology, Guilin 541004, China; 3. Key Laboratory of Marine Geographic Information Resources Development and Utilization in the Beibu Gulf, Beibu Gulf University, Qinzhou 535011, China)

**Abstract:** Karst environmental issues have become one of the hot spots in contemporary international geological research. The same problem of water shortage is one of the hot spots of global concern. The peak-cluster depression basins in southwest of Guangxi is an important water connotation and ecological barrier areas in the Pearl River Basin of China. Thus, studying the spatial and temporal variations and the influencing factors of its water yield services is critical to achieve the sustainable development of water resources and ecological environmental protection in this region. As such, this paper uses the Integrated Valuation of Ecosystem Services and Trade-offs (InVEST) model to assess the spatial and temporal variabilities of water yield services and its trends in the peak-cluster depression basins in southwest of Guangxi from 2000 to 2020. This work also integrates precipitation (Pre), reference evapotranspiration (ET), temperature (Tem), digital elevation model (DEM), slope, normalized difference vegetation index (NDVI), land use/land cover (LULC) and soil type to reveal the main factors that influence water yield services with the help of Geodetector. Results show that: 1) in time scale, the total annual water yield in the study area show a fluctuating and increasing trend from 2000 to 2020, with a growth rate of  $7.3753 \times 10^8$  m<sup>3</sup>/yr, and its multi-year average water yield was 538.07 mm; 2) in spatial pattern, with high yield areas mainly distributed in the south of the study area (mainly including Shangsi County, Pingxiang City, Ningming County, Longzhou County and Jingxi County), and low yield areas mainly distributed in Baise City and Nanning City; 3) the dominant factor of water yield within karst and non-karst land-forms is not necessarily controlled by precipitation, and the explanation degree of DEM factors in karst areas is significantly higher than that in non-karst areas; 4) amongst the climatic factors, Pre, ET and Tem are dominant in the spatial pattern of region water yield capacity. among which Pre has the highest explanatory power for the spatial heterogeneity of annual water production, with  $q$  values above 0.8, and each driver showed a significant interaction on the spatial distribution of water yield, with Pre exhibiting the strongest interaction with LULC.

**Keywords:** water yield; Integrated Valuation of Ecosystem Services and Trade-offs (InVEST); Geodetector; peak-cluster depression basins in; southwest of Guangxi, China

**Citation:** WANG Donghua, TIAN Yichao, ZHANG Yali, HUANG Liangliang, TAO Jin, YANG Yongwei, LIN Junliang, ZHANG Qiang, 2023. Evaluation and Quantitative Attribution Analysis of Water Yield Services in the Peak-cluster Depression Basins in Southwest of Guangxi, China. *Chinese Geographical Science*, 33(1): 116–130. <https://doi.org/10.1007/s11769-023-1329-1>

Received date: 2022-03-16; accepted date: 2022-06-27

Foundation item: Under the auspices of National Natural Science Foundation of China (No. 42061020), Natural Science Foundation of Guangxi Zhuang Autonomous Region (No. 2018JJA150135), Guangxi Key Research and Development Program (No. AA18118038), Science and Technology Department of Guangxi Zhuang Autonomous Region (No. 2019AC20088), The Program of Improving the Basic Research Ability of Young and Middle-aged Teachers in Guangxi Universities (No. 2021KY0431), High Level Talent Introduction Project of Beibu Gulf University (No. 2019KYQD28)

Corresponding author: TIAN Yichao. E-mail: [tianyichao1314@hotmail.com](mailto:tianyichao1314@hotmail.com)

© Science Press, Northeast Institute of Geography and Agroecology, CAS and Springer-Verlag GmbH Germany, part of Springer Nature 2023

## 1 Introduction

The supply of fresh water is an important ecosystem service that helps improve the well-being of the society and human beings (Cudennec et al., 2007). In recent decades, due to the rapid economic development and the acceleration of urbanization, the environment has been threatened, water resources in large areas have been polluted, and the pressure on groundwater resources has also increased significantly (Wada et al., 2010). Studies have shown that the number of groundwater consumers in karst formations in 2016 was approximately  $6.78 \times 10^8$ , accounting for 9.2% of the world's population (Stevanović, 2019). China has about  $3.44 \times 10^8$  km<sup>2</sup> of karst area (Jiang et al., 2014), of which the karst landform in Southwest China is the most typical, covering an area of  $4.26 \times 10^5$  km<sup>2</sup>, with a total population of more than 100 million and 48 ethnic minorities. With nearly half of the poverty-stricken population in China, Southwest China is the main poverty-stricken area in the country (Zhang et al., 2001). In karst regions, an uncoordinated two-layer spatial structure of water and soil resources has been produced due to the strong karst action, which leads to the easy surface water losses and thus causes water scarcity problems (Li Shuai et al., 2021).

The Integrated Valuation of Ecosystem Services and Trade-offs (InVEST) model was developed by the Stanford University, The Nature Conservancy (TNC) and the World Wildlife Fund (WWF). The model has been applied to many parts of the world, with relatively mature applied research abroad and has been widely used in several regions (Sánchez-Canales et al., 2012; Kovacs et al., 2013; Marquès et al., 2013). Chinese scholars have also conducted considerable research. It has been successfully applied to the assessment of water yield in lakes (Lian et al., 2019), rivers (Wei et al., 2021), the Loess Plateau (Bao et al., 2016) and Hengduan Mountains (Dai and Wang, 2020) in China. There are also scholars such as Wang Xiaofeng et al. (2020), Zuo et al. (2021) and Xia et al. (2019) quantitatively evaluated the water yield in karst areas based on the InVEST model. It is specifically manifested in geomorphological types such as Mountainous Karst (Lang and Song, 2018), depressions and tower karsts (Qi et al., 2021) and the Sancha River Basin in Guizhou (Lang et al., 2017) to provide good advice to decision makers. However, only few have quantitatively assessed the wa-

ter yield of typical karst peak-cluster depression areas. The peak-cluster depression is composed of a positive projecting rock peak and a negative depressed closed depression, the relative height difference between the peak and the bottom of the depression is between several tens and hundreds of meters (Zhu, 1982). Among them, the main factors causing the shape change of topographic units are tectonic movement, temperature, precipitation, lithology and so on. Among these factors, precipitation is the key factor in the later shaping of landform (Yang, 2019). The outer edge of the peak-cluster depression is often adjacent to the hilly plain with steep slope, wide height difference and clear boundary line. It is a special surface drought and water shortage area (Luo, 2016). In this paper, the InVEST model will be used to quantitatively assess the water yield of a typical peak-cluster depression landscape whilst selecting the key factors that affect the water yield service and analysing their quantitative impact level, which is also the focus of this paper and a problem that needs to be solved.

The quantitative analysis of the factors that affect water yield not only provides insight into the changes that occur in water yield services but also provides scientific knowledge on the mechanisms. Scholars used linear regression analysis (Xiao and Ouyang, 2019), correlation analysis (Wang X et al., 2021) and geographically weighted regression analysis (Ahmed et al., 2017) to conduct quantitative attribution analysis of water yield services. However, these analysis methods have certain limitations. For instance, they require assumptions about the premise and cannot reflect the interaction between factors objectively and effectively (Zheng et al., 2020). Changes in water yield are driven by multiple factors, and a Geodetector (Wang and Xu, 2017) can spatially satisfy the degree of correlation amongst multiple external drivers on the dynamic equilibrium of ecosystem services and is cutting-edge statistical method that cannot only characterise their degree of spatial differentiation but also build relevant regression models to detect the interaction of drivers in ecosystem services (Chen et al., 2020). Regarding the quantitative assessment of water yield using Geodetector, scholars have been working on the Beijing-Tianjin-Hebei urban agglomeration (Chen et al., 2020), the north-western North China Plain (Gao et al., 2021) and the Sanjiangyuan National Park (Wan et al., 2021) of China have been successfully ap-

plied in these regions. However, the identification of driving mechanisms for water yield services in typical peak-cluster depression basins based on Geodetector has not been applied.

The peak-cluster depression basins in southwest of Guangxi belongs to the border area of China, which is a typical representative of ‘old, young, border, mountain and poor’, and it rains a lot all year round in the watershed, with high precipitation. It is an important ecological barrier in the Pearl River Basin, as well as an important water connotation area and priority biodiversity protection area in China, and the basin has extensive rock desertification development and contains a unique double-layer hydrogeological structure of the karst landscape (Xiong et al., 2010). Therefore, it is typical and representative to select the water yield quantitative assessment and driving force analysis of the peak-cluster depression basins in southwest of Guangxi with obvious ecological fragility (Zhang et al., 2021). This paper takes the water yield service of the peak-cluster depression basins in southwest of Guangxi from 2000 to 2020 as the research object, uses the InVEST annual water yield model for visualisation and quantitative evaluation and calibrates the  $Z$ -parameter to ensure the accuracy of the results. Based on eight factors, namely, precipitation (Pre), reference evapotranspiration (ET), temperature (Tem), digital elevation model (DEM), slope, normalized difference vegetation index (NDVI), land use/land cover (LULC) and soil type, Geodetectors are used to identify and analyse the drivers of water yield services in the study area. Two main objectives are provided: 1) spatiotemporal changes and trends of water yield services in the peak-cluster depression basins in southwest of Guangxi from 2000 to 2020; and 2) quantitative analysis of single factor and interaction factor on the spatial heterogeneity of water yield services using a Geodetector. The model parameters used in this study would provide technical and methodological references for the applicability of water yield models in karst areas.

## 2 Materials and Methods

### 2.1 Study area

The peak-cluster depression basin of this study (104°56'E–108°71'E, 21°59'N–24°65'N) is located in the southwest of Guangxi Zhuang Autonomous Region (hereinafter referred to as Guangxi), China (Fig. 1). It

mainly includes most of the four prefecture-level cities of Baise, Wenshan, Pingxiang and Chongzuo, as well as some areas of Nanning and Fangchenggang. The total area is about  $6.10 \times 10^4 \text{ km}^2$ , accounting for roughly 22% of the total area of Guangxi. Its average elevation is mostly 500–1700 m. The karst landform development in the study area is typical, accounting for about 42% of the total area of the study area. Referring to related studies by scholars such as (Wu et al., 2009; Wang Shijie et al., 2013), the landform combination in this study area is dominated by peak-cluster depressions. The extraction of this study area is based on digital elevation model (DEM) and the hydrological unit area of the section above Nanning hydrological station extracted with the support of ArcGIS hydrological tools, mainly including Zuojiang, Youjiang, Yujiang and other tributaries of Xijiang River system, which governs Chongzuo, Baise, Wenshan and other areas. Based on the integrity of the basins extraction, a few areas in the southeast are in hilly plains and non-karst landscapes. The study area belongs to the southern subtropical climate (Kuang et al., 2007). The annual precipitation is 1311 mm, with abundant precipitation. The mean annual temperature is about 20°C, with sufficient light and heat. The soil types in the study area mainly include lateritic red earths, limestone soils, yellow red earths, red earths, paddy soils, yellow earths and purplish soils. Amongst which, lateritic red earths occupy the largest area, accounting for about 32%, followed by limestone soils and yellow red earths, accounting for about 23% and 16%, whilst limestone soils are mainly distributed in karst areas, respectively. Amongst the land use types, woodland and grassland account for about 87.6% of the area, followed by farmland for about 11.8%.

### 2.2 Data sources

The data required for this study include the data of water yield calculated by the InVEST model from 2000 to 2020 and the influence factor data required by Geodetector. The data required by the InVEST model include Pre, ET, root restricting layer depth, plant available water content (PAWC), LULC, plant evapotranspiration coefficient ( $K_c$ ) and root depth in biophysical table, as well as the  $Z$ -parameter. The influence factors selected by the Geodetector are Pre, ET, Tem, DEM, LULC, NDVI, slope and soil type.

The relevant basic data sources are shown in Table 1.

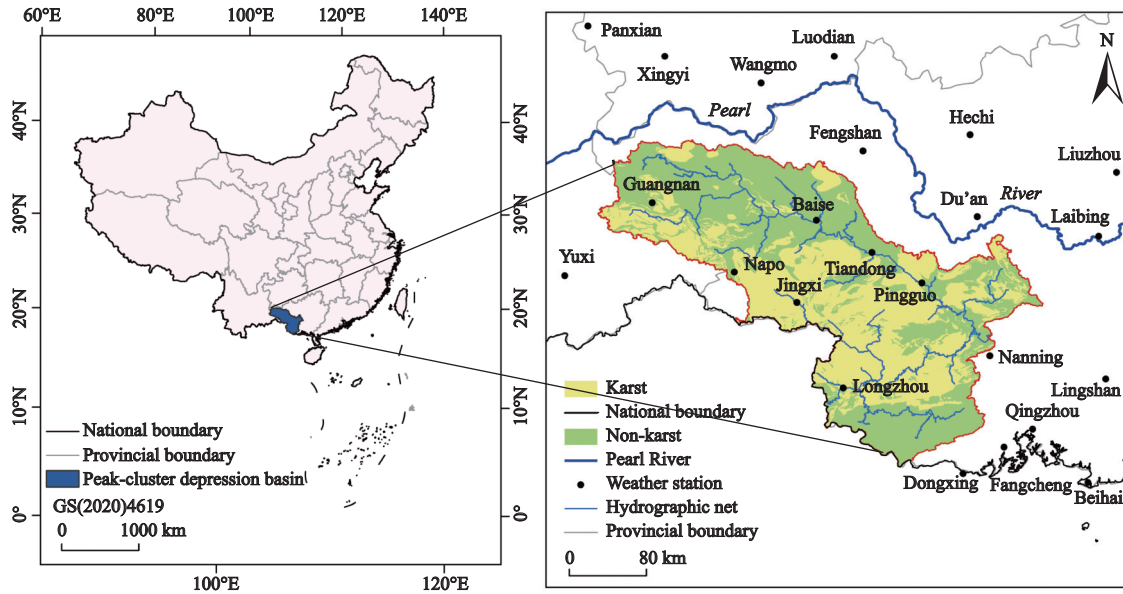


**Fig. 1** Regional overview of peak-cluster depression basins in southwest of Guangxi, China

**Table 1** Data acquisition sources for the construction of water yield model in the peak-cluster depression basins in southwest of Guangxi, China

Data	Data source and processing method	Resolution / m	Model
Pre	China Meteorological Data Network ( <a href="http://data.cma.cn/">http://data.cma.cn/</a> )	1000	Geodetector/InVEST
ET	Calculated by Penman-Monteith formula (PM)	1000	Geodetector/InVEST
LULC	MCD12Q1 data downloaded from NASA's Land Processes Distributed Active Archive Center (LP DAAC) ( <a href="https://e4ftl01.cr.usgs.gov/MOTA/MCD12Q1.006/">https://e4ftl01.cr.usgs.gov/MOTA/MCD12Q1.006/</a> )	250	Geodetector/InVEST
PAWC	Using the data in the 1 : 1 million soil map ( <a href="http://vdb3.soil.csd.cn/">http://vdb3.soil.csd.cn/</a> ), calculated in the Spaw software	1000	InVEST
Root restricting layer depth	1 : 1 million soil map ( <a href="http://vdb3.soil.csd.cn/">http://vdb3.soil.csd.cn/</a> )	1000	InVEST
Root_depth	Determined according to the reference data provided by the InVEST model	1000	InVEST
Tem	China Meteorological Data Network ( <a href="http://data.cma.cn/">http://data.cma.cn/</a> )	1000	Geodetector
DEM	Geospatial Data Cloud Website ( <a href="http://www.gscloud.cn/">http://www.gscloud.cn/</a> )	90	Geodetector
Slope	Obtained by DEM calculation in ArcGIS software	1000	Geodetector
NDVI	( <a href="https://earthexplorer.usgs.gov/">https://earthexplorer.usgs.gov/</a> )	250	Geodetector
Soil type	1 : 1 million soil map	1000	Geodetector
$K_c$	Determined according to the reference data provided by the InVEST model		InVEST
Z parameter	The model is calibrated according to the total water resources data in the 'Guangxi Water Resources Bulletin' ( <a href="http://slt.gxzf.gov.cn/zwgk/jgbg/gxszygb/">http://slt.gxzf.gov.cn/zwgk/jgbg/gxszygb/</a> ), $Z = 15.9$		InVEST

Notes: Pre is precipitation; ET is reference evapotranspiration; LULC is land use/land cover; MCD12Q1 data product is derived using supervised classifications of Moderate Resolution Imaging Spectroradiometer (MODIS) Terra and Aqua reflectance data; PAWC is plant available water content; Tem is temperature; DEM is digital elevation model; NDVI is normalized difference vegetation index;  $K_c$  is plant evapotranspiration coefficient

Amongst them, the meteorological data (e.g., Pre, ET, Tem) were obtained from the data of the study area and its surrounding meteorological stations in the same period, and the meteorological raster data were produced with the help of ArcGIS10.7 spline method interpolation technique. LULC, NDVI and DEM data were mosaicked with the help of ArcGIS 10.7 after download-

ing. The above data are based on the above operations and then uses the GIS clipping tool to make the corresponding data for the study area. Based on the basic data of the 1 : 1 million Chinese soil database produced by the Nanjing Institute of Soil Research, Chinese Academy of Sciences, this paper calculates the PAWC, root restricting layer depth and the soil type data. All the afore-

mentioned data are resampled into a spatial resolution of 1000 m, the projection type is UTM 48 N, and the central longitude is 108°E.

## 2.3 Methods

### 2.3.1 InVEST water yield model

The annual water yield of this study is based on precipitation, reference evapotranspiration, land use/land cover, plant available water content and root restricting layer depth run in InVEST version 3.9.0:

$$Y(x) = (1 - AET(x)/P(x)) \times P(x) \quad (1)$$

where  $Y(x)$  is the annual water yield (mm) of each grid cell  $x$ ,  $AET(x)$  is the actual annual evapotranspiration (mm) of each grid cell  $x$ , and  $P(x)$  is the annual precipitation (mm) for each raster cell  $x$ , where  $AET(x)/P(x)$  is calculated as:

$$AET(x)/P(x) = 1 + PET(x)/P(x) - (1 + (PET(x)/P(x))^\omega)^{1/\omega} \quad (2)$$

where  $AET(x)/P(x)$  is the vegetation evapotranspiration of LULC; and  $PET(x)$  is the potential evapotranspiration, and the calculation formula is expressed as follows:

$$PET(x) = K_c(l_x) \times ET_0(x) \quad (3)$$

where  $K_c(l_x)$  is the vegetation evapotranspiration coefficient of LULC in each raster cell  $x$ , and  $ET_0(x)$  is the reference evapotranspiration for each raster cell  $x$ .

$\omega(x)$  is an empirical parameter, and its calculation formula is expressed as follows:

$$\omega(x) = Z \times AWC(x)/P(x) + 1.25 \quad (4)$$

where  $AWC(x)$  is the annual average plant available water content for each grid cell  $x$ ,  $Z$  is the seasonal constant, and 1.25 is the cardinality of  $\omega(x)$ .

### 2.3.2 Geodetector

Geodetector is a statistical method used for detecting the spatial heterogeneity of matter and its driving factors. It is divided into four modules, namely, factor detector, in-

teraction detector, risk zone detector and ecological detector. In this paper, we mainly use factor and interaction detectors for further analysis.

#### (1) Factor detector

This module detects the spatial heterogeneity of water yield, and the degree of explanation of the eight factors of Pre, ET, Tem, DEM, Slope, NDVI, LULC and Soil type to the spatial heterogeneity of water yield, measured by the  $q$  value, and its expression is

$$q = 1 - \sum_{h=1}^L N_h \sigma_h^2 / N \sigma^2 \quad (5)$$

where  $h$  is the stratification status of the dependent variable water yield or the independent variable Pre, ET, Tem, DEM, Slope, NDVI, LULC and Soil type;  $L$  is the number of layers and there are  $L$  layers in total;  $N_h$  and  $N$  are the number of cells within the  $h$ -tier and in the whole region, respectively;  $\sigma_h^2$  and  $\sigma^2$  are the variances of the dependent variable water yield within the  $h$ -stratum and for the whole region, respectively.

#### (2) Interaction detector

This module identifies whether the explanation degree of dependent variable water yield will increase or decrease when two independent variables  $X1$  and  $X2$  act together. The interaction types are shown in the table below (Table 2).

#### (3) Selection and pre-treatment of impact factors

With reference to related research (Gao et al., 2020; Hu et al., 2020; Wang H et al., 2021), this article selected 8 independent variables as influencing factors (Fig. S1). The spatial heterogeneity of water yield is analysed and pre-processed with reference to the data discretization method and experience proposed by (Wang and Xu, 2017): grading NDVI, DEM, ET, Pre and Tem data according to the natural breakpoint method, where NDVI data are classified into seven levels, and the remaining data are classified into nine levels; slope data are divided into six levels according to  $\leq 5^\circ$ ,  $5^\circ-8^\circ$ ,

**Table 2** Types of interaction between two covariates of the Geodetector

Criterion	Interaction
$q(X1 \cap X2) < \min(q(X1), q(X2))$	Non-linear, weaken
$\min(q(X1), q(X2)) < q(X1 \cap X2) < \max(q(X1), q(X2))$	Single factor, non-linear, weaken
$q(X1 \cap X2) > \max(q(X1), q(X2))$	Two-factor, enhancement
$q(X1 \cap X2) = q(X1) + q(X2)$	Independent
$q(X1 \cap X2) > q(X1) + q(X2)$	Non-linear, enhancement

8°–15°, 15°–25°, 25°–35° and >35°; both LULC and Soil type data are type quantity data and do not need to be processed.

### 2.3.3 Theil-Sen trends

In this paper, the Theil-Sen trend analysis method is applied for the analysis of water yield time series with the help of MATLAB2009a software, and the Theil-Sen trend value and the spatial distribution map of significant changes in Theil-Sen trend in the study basin are obtained, which can intuitively and effectively reflect the spatial distribution trend characteristics of water yield in peak-clusters depressions basins in southwest of Guangxi from 2000 to 2020 and the significance level of water yield trend change in the study area, the calculation formula is expressed as follows:

$$\rho = \text{median}\left(\frac{x_j - x_i}{j - i}\right), 1 < i < j < n \quad (6)$$

where  $\rho$  is the Sen trend degree;  $x_j$  and  $x_i$  are the time series of water yield. When  $\rho < 0$ , the water yield of time series shows a downward trend, and when  $\rho > 0$ , the time series is showing an upward trend.

## 3 Results

### 3.1 Characteristics of interannual variation in water yield

From 2000 to 2020, the average annual total water yield of peak-cluster depression basins in the southwest of Guangxi (Fig. 2) showed a fluctuating and increasing trend, the trend slope was  $7.38 \times 10^8 \text{ m}^3/\text{yr}$ , and the average total water yield in 21 yr was  $330.00 \times 10^8 \text{ m}^3$ . The total average annual water yield ranged from  $154.00 \times 10^8$  to  $582.00 \times 10^8 \text{ m}^3$ , with the lowest value occurring in 2004 ( $154.85 \times 10^8 \text{ m}^3$  produced) and the highest value in 2017 ( $582.51 \times 10^8 \text{ m}^3$  produced). In general, the changes in the total water yield of the peak-cluster depression basins in southwest of Guangxi from 2000 to 2020 can be roughly divided into four stages: a downward trend from 2001 to 2004; a fluctuating upward trend from 2005 to 2009; and an upward trend from 2010 to 2017 status; and 2017 to 2020 shows a downward trend again.

Fig. 3 shows the interannual trends of multi-year average Pre, ET and water yield in the peak-cluster depression basins in southwest of Guangxi from 2000 to 2020. During that period, the average multi-year Pre in the study area was 1311.63 mm, which was gradually

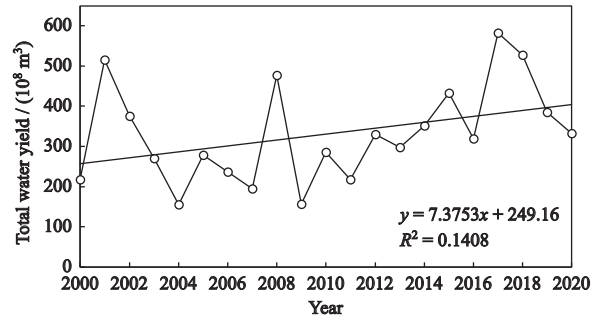


**Fig. 2** Trends in total water yield from 2000 to 2020 in the peak-cluster depression basins in southwest of Guangxi, China. The total water yield ( $\text{m}^3$ ) equals water yield (mm) multiplied by area

increasing overall with a linear trend of 10.56 mm/ yr. This finding is consistent with the results in Huanjiang Maonan Autonomous County in Guangxi, which also has a subtropical climate, where Pre has a tendency to increase with annual Pre between 2006 and 2010 (Chen et al., 2012), the lowest multi-year average Pre occurred in 2004 (993.14 mm) and the highest in 2017 (1702.26 mm); the multi-year average ET was 1069.35 mm, with a slightly decreasing linear trend of  $-2.03 \text{ mm/ yr}$  from 2000 to 2020, which is consistent with the results in a typical karst area, Guilin City, Guangxi, where the ET also showed a significant decreasing trend with a rate of  $-8.02 \text{ mm}/10\text{yr}$  between 1951 and 2015 (Guo et al., 2019), the lowest value of multi-year average ET appeared in 2017 (979.35 mm), and the highest value appeared in 2003 (1129.99 mm); the multi-year average water yield was 538.07 mm, which accounts for 41% of the Pre, and the trend during the study period remained largely consistent with the average annual Pre, with a linear increasing trend of 10.43 mm/yr, the lowest value of multi-year average water yield appeared in 2004 (252.35 mm), and the highest value appeared in 2017 (949.26 mm). Overall, Pre and water yield showed an increasing trend, with Pre increasing slightly greater than water yield, whilst ET showed a slight decreasing trend.

### 3.2 Spatial analysis of water yield

The spatial distribution of annual water yield in the peak-cluster depression basins in southwest of Guangxi from 2000 to 2020 exhibits strong spatial heterogeneity. The interannual variation of water yield in the basin is large, but its spatial distribution is basically consistent, showing a pattern of high in south and low in north. Based on the natural breakpoint classification, the annual water yield was reclassified into seven classes (Fig. 4). As

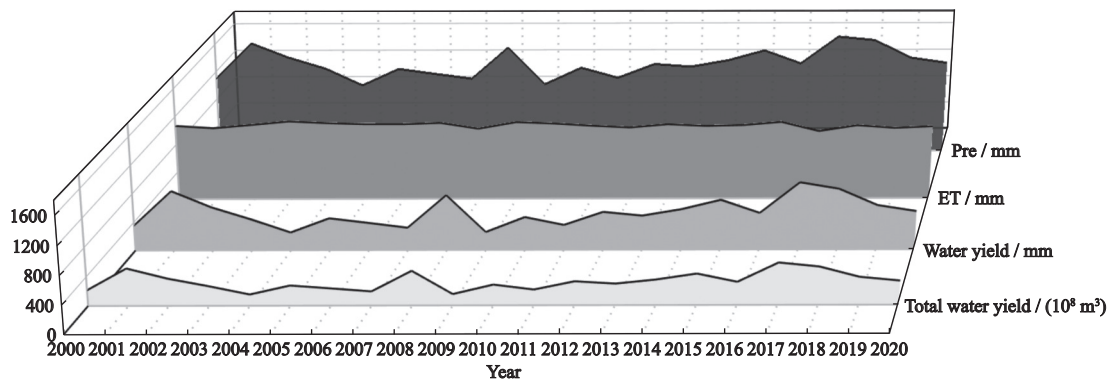


**Fig. 3** Precipitation (Pre), reference evapotranspiration (ET), and water yield (WY) in the peak-cluster depression basins in southwest of Guangxi, China

seen in Fig. 4, in 2000–2015, the high-yield water area is located in the southeast (Shangsi County, Fangchenggang). This area has abundant Pre, the soil type is mostly lateritic red earths, and the water content is low (Chen, 1989), thereby making the area a high water yield. The low-yield water areas are located in the northwest (Baise City, and its Xilin County, Tianyang County, Lingyun County, Tianyang County), the middle east (Nanning City and Fusui County), may be due to the low precipitation in this part of the region, and its soil type is mostly yellow soil, the soil moisture content is high (Jiang et al., 2006), which makes the actual evapotranspiration of the region greatly increased, resulting in low water yield. From 2016 to 2020, the high-yield water area tends to the southwest (Pingxiang City, Ningming County, Longzhou county and Jingxi County), due to the increase in Pre in the region, and its soil types are mostly lateritic red earths and purplish soils, with low soil moisture content (Chen, 1989; Hu et al., 2017); most of the low-yield water areas are still located in the northwest (Baise area) and the middle east (Nanning City).

Spatial overlay of the Theil-Sen trend values and significance level  $P$ -values yield five categories: significant increased, moderate increase, slight increase, slightly decrease, and seriously decrease. Fig. 5 shows that the area occupied by the area of increased water yield is significantly larger than that of decreased area, accounting for 95.60% of the total area of the study area, whilst the decreased area only accounts for 4.40%. Specifically, the area with a significant increase in annual water yield accounts for 8.53%, which is mainly distributed in Pingxiang City, Longzhou County and Ningming County in the south to west part of the study area; moderately

increasing areas accounted for 49.99% and slightly increasing areas accounted for 37.08%, with the largest proportion of these two components concentrated in the three prefectures of Chongzuo, Baise and Nanning cities in the study area; slightly decreasing areas account for 4.11% and are mainly embedded in slightly increasing areas; severely reduced areas accounted for 0.28%, mainly concentrated in Fangchenggang City.

### 3.3 Response of water yield to the main influencing factors

#### 3.3.1 Detection analysis of dominant influence factors on water yield

In this paper, the basin water yield is taken as the dependent variable, and each influencing factor is taken as the independent variable. In the calculation process, this paper resampled all data in ArcGIS software to the spatial resolution of 8000, 5000 and 2000 m for experiments to ensure the accuracy of the calculation results.

The test process is as follows: the first step is to reclassify the water yield data and sample it as point data; the second step is to reclassify the influencing factors into category variable; the third step is to resample the results of step two with the results of step one; the fourth step is to input the final table data generated by step three into the geographic detector software compiled by Excel to obtain the final result. Whilst the Geo-detector software prepared by Excel will have higher accuracy of calculation results if the density of grid point data is larger, the calculation volume will also be larger (Chen et al., 2020). Through experiments, in the pursuit of a balance between the accuracy and efficiency of the calculation results, we selected the data with 15 367 grid points and 2000 m spatial resolution.

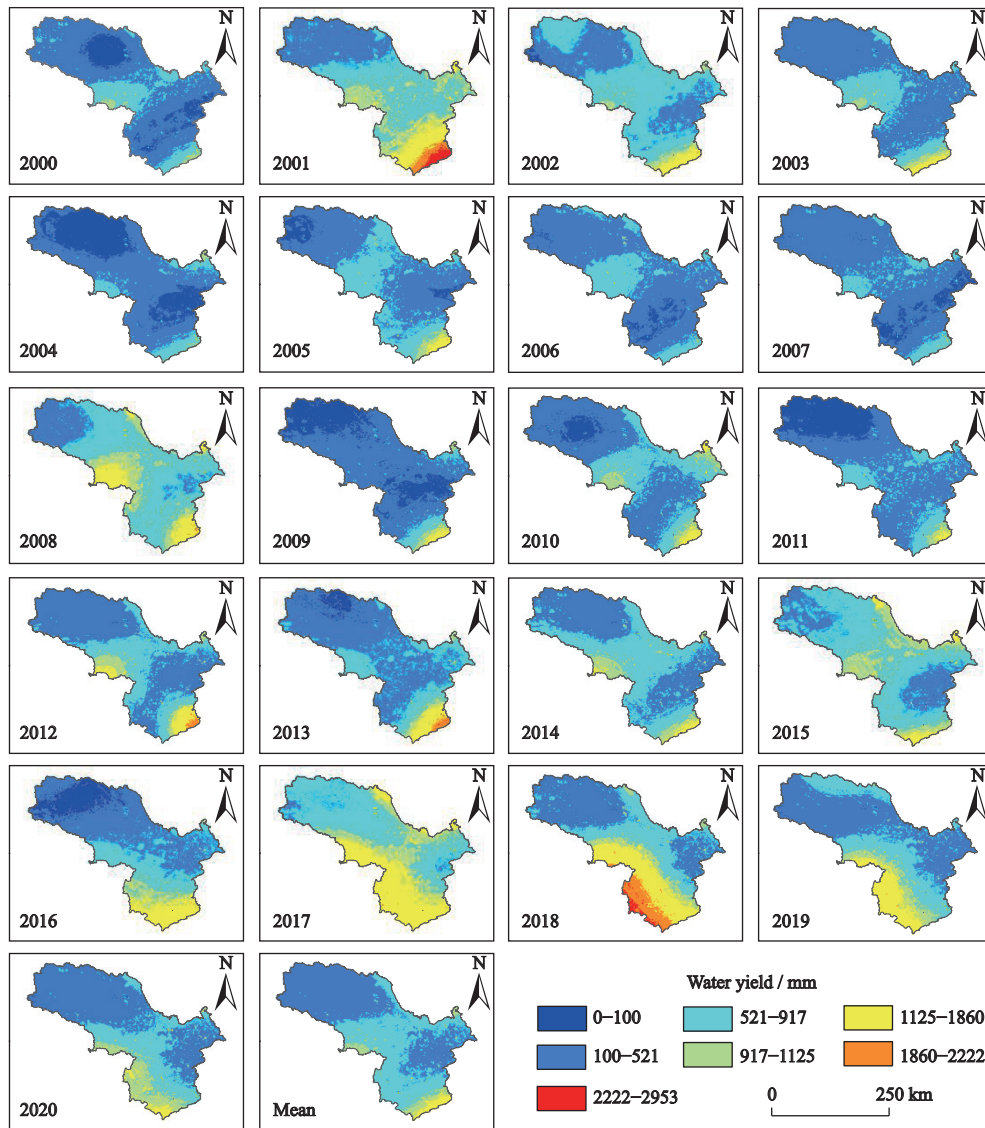


Fig. 4 Spatial distribution of water yield in the peak-cluster depression basins in southwest of Guangxi, China from 2000 to 2020

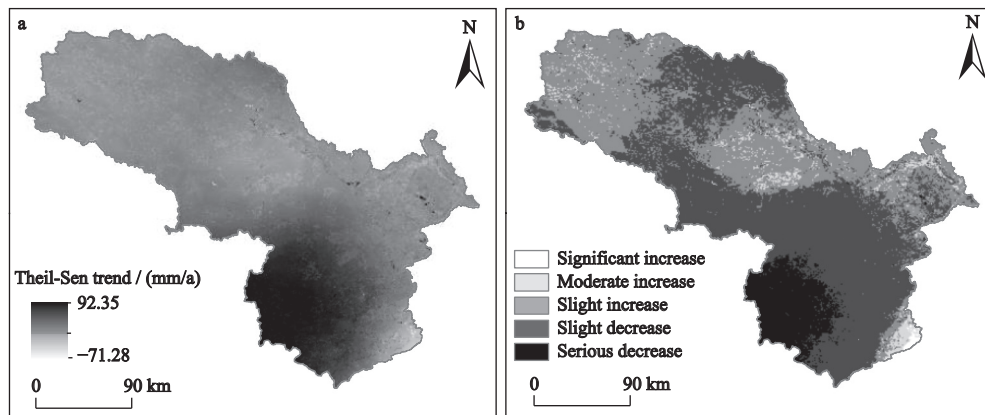


Fig. 5 The spatial variation of Sen trend (a) and significance analysis of variation trend (b) of water yield in the peak-cluster depression basins in southwest of Guangxi, China from 2000 to 2020



The larger the  $q$ -value of the single factor detection of the Geodetector is, the higher the degree of spatial heterogeneity explained by the factor in terms of water yield, the greater the degree of correlation between the factor and annual water yield. In this study, the annual water yield in 2000, 2005, 2010, 2015 and 2020 were selected for the factor detection analysis (Fig. 6). Pre explained the highest spatial heterogeneity in annual water yield throughout the study area, with  $q$  values above 0.8 for each year. Followed by ET and Tem, the study found that the spatial distribution of annual water yield in the study area in 2000 and 2020 was only second to Pre in correlation with ET in the five years, in which the factor detection analysis was conducted, whilst the spatial heterogeneity of Tem on annual water yield services was stronger than that of ET to explain it in 2005, 2010 and 2015. Due to special factors, such as geographical location and landform, obvious differences in temperature changes in the basin are observed, and a sudden increase in the annual average temperature in Guangxi around 2001 (Wang Ying et al., 2013) may have a certain impact on the spatial pattern of water yield. The next factors with an explanatory power of 10%–20% are DEM, LULC and soil type, amongst which Soil type has the strongest explanatory power, indicating that the physical and chemical properties of the soil also have some influence on the spatial distribution of water yield. NDVI and slope have the lowest contribution to the annual water yield of the basin.

### 3.3.2 Dominant factors of water yield in different landform types

Further, the single factor detector is used to detect and analyze the water yield in different karst and non-karst

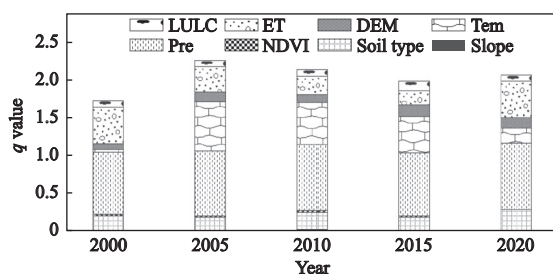


**Fig. 6** Single-factor explanatory degree ( $q$  value) of water yield influence factors for 2000, 2005, 2010, 2015 and 2020 in the peak-cluster depression basins in southwest of Guangxi, China. LULC is land use/land cover; ET is reference evapotranspiration; DEM is digital elevation model; Tem is temperature; Pre is precipitation; NDVI is normalized difference vegetation index

landform types in the study area. The operation results show that there are significant differences in the response of the same factor to the spatial differentiation of water yield in different landform types (Fig. 7). As shown in Fig. 7, Pre is still the most important factor affecting water yield within non-karst landscapes, which is consistent with previous studies in non-karst landscapes such as the Beijing-Tianjin-Hebei urban agglomeration (Chen et al., 2020), the Beijing ecological red line area (Gao et al., 2020), and the Yellow River Basin (Li G Y et al., 2021). While the dominant factor within the karst landscape was DEM in 2000 and ET in 2015, the dominant factor in the remaining three years was Pre, indicating that the dominant factor of water yield in the karst landscape was not necessarily controlled by Pre in different years. However, the most obvious result of factor detection analysis within different geomorphological types is that the interpretation degree of DEM factors in karst areas is higher than that in non-karst areas. This phenomenon may be due to the fact that the typical karst peak-cluster depression area in this study area has a large elevation variation, with many steep-slope peak-cluster mountains, tall mountains, and obvious vertical bands of mountains (Luo, 2016). With the change of altitude, climate, Pre and topography are more significant with elevation changes, and thus the spatial heterogeneity of water yield is more obvious. The responses of the remaining factors to the different landform type zones are consistent with the detection results within the whole region.

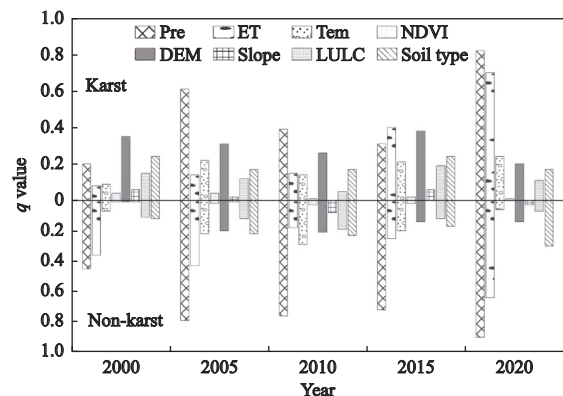


**Fig. 7** Univariate explanatory degree ( $q$  value) of water yield in 2000, 2005, 2010, 2015, 2020 in karst and non-karst different landform type zones in southwest of Guangxi, China. Pre is precipitation, ET is reference evapotranspiration; Tem is temperature; NDVI is normalized difference vegetation index; DEM is digital elevation model; LULC is land use/land cover

### 3.3.3 Interaction analysis of influencing factors of water yield

The degree of influence of individual factors on the spatial distribution of water yield services was analysed, but in reality, it is a complex ecological process driven by multiple factors. This paper selects water yield services in 2000, 2005, 2010, 2015 and 2020 for interactive detection analysis (Fig. 8). The results of the interaction detectors further support this view, the spatial interactions among the factors influencing the annual water yield service in the peak-cluster depression basins in southwest of Guangxi are all greater than the explanatory degree of any single factor for the annual water yield, and the interaction types are a combination of nonlinear and two-factor enhancements, with the nonlinear enhancement interaction being more significant. In Fig. 7, Pre has the strongest effect on the spatial pattern of water yield, with a strong significant interaction with any of the influencing factors. In 2000, 2005, 2010, 2015 and 2020, Pre has the strongest interaction with LULC and a slightly weaker interaction with soil type, but the overall explanatory degree is above 0.82; the in-

teraction of ET with Tem was slightly weaker than the interaction of Pre with either factor; the interaction among LULC, NDVI, slope and soil type is weak, except that the interaction between LULC and Soil type is slightly stronger, and the other values are below 0.30.

## 4 Discussion

### 4.1 InVEST annual water yield model calibration and evaluation

The accuracy and validity of the calculated results using the model depend on the value of Z-parameter to a large extent whilst ensuring that the input parameters are correct. Z-parameter is an empirical constant that represents Pre distribution and other hydrological address characteristics in the study area, with a value range of 0–30. However, as an empirical constant of Z-parameter, the choice of its value is uncertain. Subsequently, to select the appropriate parameter value, the method of choosing Z-parameter should be known to make the optimal choice. At present, the calculation methods of Z-parameter are as follows: 1) according to

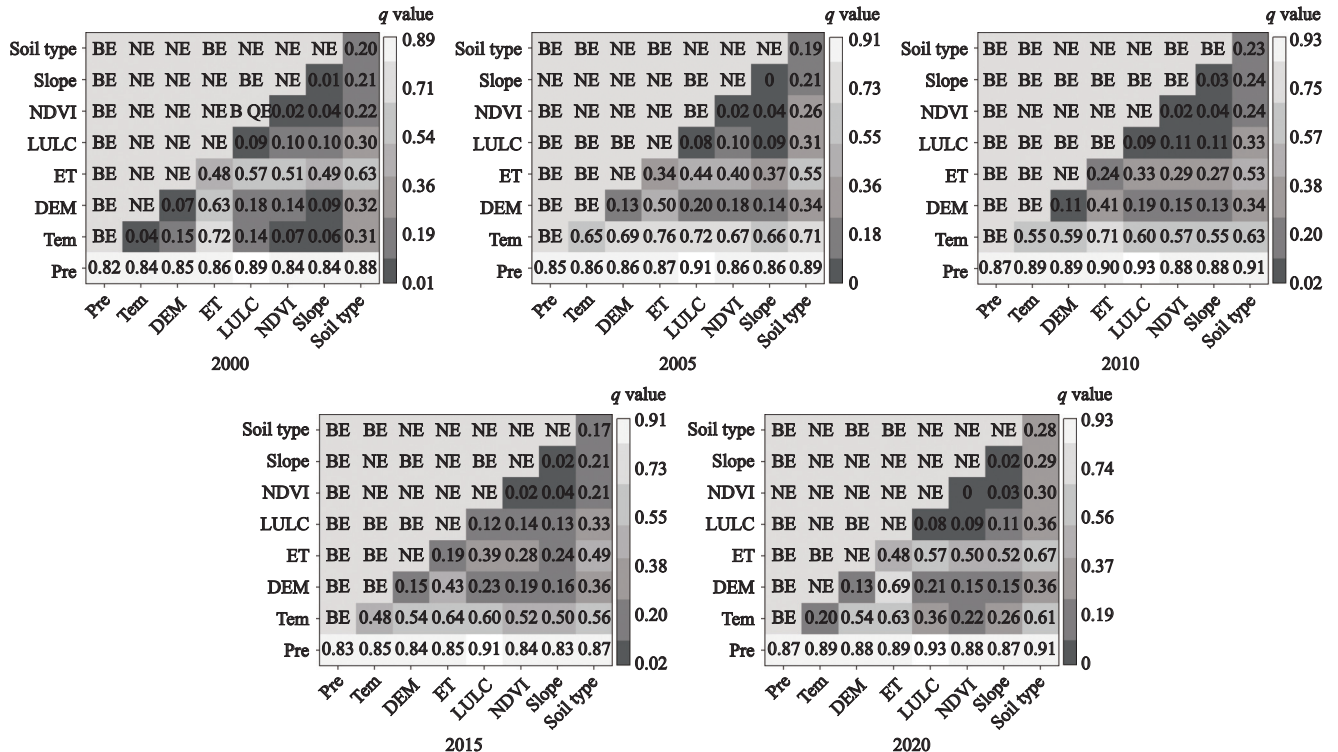


Fig. 8 Detected results of the interaction of the influencing factors of water yield in the peak-cluster depression basins in southwest of Guangxi in 2000, 2005, 2010, 2015, and 2020. Pre is precipitation; Tem is temperature; DEM is digital elevation model; ET is reference evapotranspiration; LULC is land use/land cover; NDVI is normalized difference vegetation index; NE represents non-linear; enhancement; Be means two-factor, enhancement

$\omega$  empirical data, about  $\omega$  there are many relevant studies on empirical values (Xu et al., 2013; Liang and Liu, 2014), and the  $Z$ -parameter can be calculated according to Eq. (4); 2) according to the formula developed by (Donohue et al., 2012):  $Z = 0.2 \times N$ , and  $N$  represents the number of precipitation events per year. 3) using the actual total amount of water resource data for calibration, total water resource refers to the total amount of surface and underground water yield formed by local Pre during the year, excluding transit water. Among them, the shallow underground water yield in the hilly area of Guangxi is the river base flow, which is the repeated calculation amount, and the final total water resource is equal to the sum of the surface water resource and the non-duplicated groundwater resource (Pan and Jin, 1996). In terms of total conservation, the water yield and the total water resource are essentially calculations of the same resource using different methods (Wang Baosheng et al., 2020). Considering that the first two calculation methods calculate the  $Z$ -parameter with the input of empirical values, the calculation results of the model cannot guarantee obtaining a very good accuracy. Hence, this study calculates the  $Z$ -parameter by using a third approach. However, the boundary of this study area is not completely consistent with the boundary of districts and counties, and the water resource data of the administrative areas cannot be used directly. Therefore, this study uses the total water resources of the four administrative divisions of Baise, Chongzuo,

Nanning and Fangchenggang provided in the Guangxi Water Resources Bulletin. The quantity data are converted into the quantity of water resources per unit area, the calculated water resources per unit area of the above four administrative regions is 601.7 mm, and when  $Z = 15.9$ , the water yield per unit area of this study area is 575.0 mm, and the relative error is controlled within 4.4%, which shows that the simulation results are good.

According to the estimation results, the multi-year average water yield of the study area from 2000 to 2020 is 538.07 mm, and the spatial differentiation in the basin, which is related to the geographical location of the basin, is significant. The study area is located on the slope of the transition from the Guizhou plateau to the Guangxi basin, thereby straddling the humid central subtropical climate and the humid southern subtropical climate according to the climatic zoning of China (Zheng et al., 2010). Judging from the results of previous studies (Table 3), with the increase in Pre in the study areas belonging to temperature zones, such as mid-temperate, warm-temperate, north subtropical, mid-subtropical, south subtropical and tropical temperature zones, the water yield also tends to increase. The regional average annual water yield is greater than the annual water yield (502 mm) of Baoshan City (Chen et al., 2021), which straddles the central and southern subtropics, and less than the average annual water yield of the tropical Hainan Island (980 mm and 1024 mm) (Wu et al., 2013; Han et al., 2022), which can prove the credib-

**Table 3** Comparison of water yield of each study area divided according to China's climate region

Climate zone	Study area	$Z$ -parameter	Pre / (mm/yr)	Water yield / (mm/yr)	References
Mid-temperate zone	Shiyang River Basin	Calibrated	222	61	(Wang et al., 2018)
Across the mid-temperate zone and warm-temperate zone	Yellow River Basin	Calibrated	200–650	74	(Yang et al., 2020)
Across the mid-temperate zone and warm-temperate zone	Agro-pastoral ecotone of northern China	Assign a value of 30	418	97	(Pei et al., 2021)
Warm-temperate zone	Qinling Basin	Calibrated	791	236	(Li et al., 2021c)
North subtropical climate	Jianghuai ecological economic zone of China	$\omega$ Empirical data	1013	363	(Guo et al., 2021)
North subtropical climate	Taihu Lake Basin	No calibration	1219	742	(Gu et al., 2018)
Mid-subtropical climate	Wujiang River Basin	Assign a value of 1	1061	549	(Xia et al., 2019)
Mid-subtropical climate	Sancha River Basin	No calibration	> 1000	643	(Gao and Wang, 2019)
Across the Mid-subtropical and southern subtropical climates	Baoshan City	No calibration	1478	502	(Chen et al., 2021)
Tropical climate	Hainan Island	Calibrated	1500	980	(Wu et al., 2013)
Tropical climate	Hainan Island	Calibrated	1930	1024	(Han et al., 2022)

ility of the results of this paper. The slight differences are mainly due to two factors: one of them is the differences in data sources, data spatial resolution and meteorological data interpolation methods used by different scholars, and the second is the different values of Z-parameters. Although the estimation of water yield based on the InVEST model has been applied globally by various scholars, there are empirical formulas in the selection of parameters in the model. Thus, the water yield calculated by different scholars will inevitably produce certain deviations. Even though the same model is used in the same region, significant differences may still be observed in the results calculated by different scholars.

#### 4.2 Analysis on dominant factors of water yield

Water yield is an important regulating service of ecosystem services (Li Li et al., 2021). Hence, the identification of its spatial heterogeneity and influencing factors are not only important elements in the study of ecosystem services but also a scientific basis for evaluating the regional resource and environmental carrying capacity and territorial spatial planning. The driving factors that affect the spatial distribution of water yield include topographic factors, meteorological factors, vegetation factors and human activities. In this paper, a single-factor quantitative analysis of the spatial heterogeneity of water yield was conducted with the help of a Geodetector, and the results show that Pre has the highest explanatory power for water yield in this study area, which is consistent with a series of recent research results published by previous authors (Chen et al., 2020; Wang T H et al., 2020). Although the research methods used by other scholars for the analysis of the drivers of water yield differ (Wang T H et al., 2020; Li M Y et al., 2021), they basically achieve consistent conclusions, thereby proving the reliability of the results of this paper.

In this paper, we further analyzed the water yield within the karst and non-karst landscape types in the study area, and the most obvious result of the analysis is that the explanation degree of DEM factors in the karst area is higher than that in the non-karst area. peak-cluster depression landform is a special landform formed at a certain stage of karst landform development. It is a type of karst with the most distinctive topographic features, the most diverse forms, the most peculiar landscape, the strongest karst action, the most complicated

hydrogeological conditions and the most complete generation system. This landform type is mainly affected by the dissolution of Pre and the development of fissures along the geological and tectonic movements (Yang, 2019). In this study area, the peaks and clusters are densely covered with depressions, the slope of the terrain is also relatively large, the rocky peaks are tall and straight, and the landform development is relatively active. Elevation significantly affects Pre and the distribution of vegetation types, and therefore can indirectly affect water yield capacity (Wang Xiuming et al., 2020).

This paper analyses the interaction detection and analysis of the spatial pattern of water yield. The results show that the interaction types are two-factor enhancement and non-linear enhancement, and the interaction between Pre and LULC had the greatest influence and the strongest explanatory power, which is consistent with the analysis results in Huang et al. (Huang et al., 2021) and Wang et al. (Wang Xiuming et al., 2020) on the Shiyang River Basin and Shaoguan City, Guangdong Province, respectively. This finding is also reflected in the research directions in recent years, where many scholars (Belete et al., 2020; Wei et al., 2021) tend to explore the impact of regional land use changes on water yield, indicating that meteorological factors largely determine the spatial differences of water producing ecosystem service functions, and land use type is the main factor that affects its spatial distribution.

#### 4.3 Uncertainty analysis and future research directions

Although the InVEST model has been widely used all over the world, its water yield assessment module does not consider the impact of complex terrain, land underlying surface geographical environment and groundwater on water yield (Sharp et al., 2014). Moreover, the input and setting of model parameters are particularly important. The data root restricting layer depth of the soil and the data in the biophysical table used in this paper were obtained from the reference data provided by China soil database and the InVEST model, as well as the uncertainty caused by the interpolation method of input meteorological data, LULC and Z-parameters. Although this model does not affect the basic pattern of water yield in the study area, it affects the accuracy of the results to a certain extent. Furthermore, in this study, we only discussed the main factors that have an impact

on water yield, whilst the specific mechanisms of each factor on water yield were not investigated in depth. In conclusion, although the results in this paper are as close as possible to the actual total water resources after several simulations and the interannual variability of the long time series is added to increase the credibility of the results, the correction of all input parameters and the specific response mechanism of each factor to the water yield service are not considered, and this aspect is a key research direction for the future.

## 5 Conclusions

Based on the InVEST model, this paper quantitatively and qualitatively analyzed the ecological service system of water yield in the peak cluster depression basin in southwest of Guangxi from 2000 to 2020, and further quantified the response between water yield and various influencing factors in the basin. During the monitoring period, the annual water yield in the study area showed an increasing trend year by year, which was  $7.3753 \times 10^8 \text{ m}^3/\text{yr}$ . Among them, the water yield of the southeast (Shangsi County, Fangchenggang) and southwest (Pingxiang City, Ningming County, Longzhou County, Jingxi County) of the study area is about 1500 mm and above, which is a high-yield water area; the northwest (Baise City) and east-central (Nanning City) near the water yield between 0–500 mm, low water yield area. However, the water yield of Shangsi County, located in the southeast, has been declining in recent years, and the local government needs to give sufficient attention and priority protection. In terms of quantitative analysis of driving factors, the spatial heterogeneity between Pre and water yield in the study area is the strongest, and the interactive detection results of any influencing factor and Pre have strong spatial heterogeneity, among which the interaction with LULC is the strongest. The development of this study is expected to provide advice on water resources management for the peak cluster basin in southwest of Guangxi, and has certain reference significance for the evaluation of water production services in karst areas of China.

## Appendix

Fig. S1 could be found in the corresponding article at <http://egeoscienc.neigae.ac.cn/article/2023/1>.

## References

- Ahmed M A A, Abd-Elrahman A, Escobedo F J et al., 2017. Spatially-explicit modeling of multi-scale drivers of aboveground forest biomass and water yield in watersheds of the Southeastern United States. *Journal of Environmental Management*, 199: 158–171. doi: [10.1016/j.jenvman.2017.05.013](https://doi.org/10.1016/j.jenvman.2017.05.013)
- Bao Yubin, Li Ting, Liu Hui et al., 2016. Spatial and temporal changes of water conservation of Loess Plateau in northern Shaanxi province by InVEST model. *Geographical Research*, 35(4): 664–676. (in Chinese)
- Belete M, Deng J S, Abubakar G A et al., 2020. Partitioning the impacts of land use/land cover change and climate variability on water supply over the source region of the Blue Nile Basin. *Land Degradation & Development*, 31(15): 2168–2184. doi: [10.1002/ldr.3589](https://doi.org/10.1002/ldr.3589)
- Chen Hongsong, Yang Jing, Fu Wei et al., 2012. Characteristics of slope runoff and sediment yield on karst hill-slope with different land-use types in northwest Guangxi. *Transactions of the Chinese Society of Agricultural Engineering*, 28(16): 121–126. (in Chinese)
- Chen J, Wang D, Li G et al., 2020. Spatial and temporal heterogeneity analysis of water conservation in Beijing-Tianjin-Hebei urban agglomeration based on the Geodetector and spatial elastic coefficient trajectory models. *Geohealth*, 4(8): e2020GH000248. doi: [10.1029/2020GH000248](https://doi.org/10.1029/2020GH000248)
- Chen Meihua, 1989. Water retentivity for low retentive section of red soil in south Guangxi. *Southwest China Journal of Agricultural Sciences*, 2(3): 61–65. (in Chinese)
- Chen Wenhua, Xu Juan, Li Shuangcheng, 2021. Water conservation function of mountainous city in western Yunnan: a case study of Baoshan City. *Acta Scientiarum Naturalium Universitatis Pekinensis*, 57(6): 1153–1160. (in Chinese)
- Cudenne C, Leduc C, Koutsoyiannis D, 2007. Dryland hydrology in Mediterranean regions—a review. *Hydrological Sciences Journal*, 52(6): 1077–1087. doi: [10.1623/hysj.52.6.1077](https://doi.org/10.1623/hysj.52.6.1077)
- Dai Erfu, Wang Yahui, 2020. Spatial heterogeneity and driving mechanisms of water yield service in the Hengduan Mountain region. *Acta Geographica Sinica*, 75(3): 607–619. (in Chinese)
- Donohue R J, Roderick M L, McVicar T R, 2012. Roots, storms and soil pores: incorporating key ecohydrological processes into Budyko's hydrological model. *Journal of Hydrology*, 436–437: 35–50. doi: [10.1016/j.jhydrol.2012.02.033](https://doi.org/10.1016/j.jhydrol.2012.02.033)
- Gao J B, Jiang Y, Wang H et al., 2020. Identification of dominant factors affecting soil erosion and water yield within ecological red line areas. *Remote Sensing*, 12(3): 399. doi: [10.3390/rs12030399](https://doi.org/10.3390/rs12030399)
- Gao J B, Jiang Y, Anker Y, 2021. Contribution analysis on spatial tradeoff/synergy of karst soil conservation and water retention for various geomorphological types: geographical detector application. *Ecological Indicators*, 125: 107470. doi: [10.1016/j.ecolind.2021.107470](https://doi.org/10.1016/j.ecolind.2021.107470)
- Gao Jiangbo, Wang Huan, 2019. Spatio-temporal tradeoff of Karst water yield and soil erosion based on GWR Model: a case study in Sancha River Basin of Guizhou Province, China.

- Mountain Research*, 37(4): 518–527. (in Chinese)
- Guo Jinyi, Li Yiping, Du Wei, 2018. Evaluation on water source conservation capacity and analysis of its variation characteristics of Taihu Lake Basin based on InVEST model. *Water Resources Protection*, 34(3): 62–67. (in Chinese)
- Guo M, Ma S, Wang L J et al., 2021. Impacts of future climate change and different management scenarios on water-related ecosystem services: a case study in the Jianghuai ecological economic Zone, China. *Ecological Indicators*, 127: 107732. doi: 10.1016/j.ecolind.2021.107732
- Guo Xiaojiao, Gong Xiaoping, Shi Jiansheng et al., 2019. The temporal variations of potential evapotranspiration and influence factors for a typical karst area. *Acta Geologica Sinica*, 93(12): 3269–3281. (in Chinese)
- Han Nianlong, Zhang Yiqing, Zhang Weixuan, 2022. Simulation of temporal and spatial changes of land use and water yield in Hainan Island. *Water Resources Protection*, 38(2): 119–127. (in Chinese)
- Hu Chuanwang, Wang Hui, Liu Chang et al., 2017. Difference analysis of hydraulic characteristics of typical soils in south China. *Journal of Soil and Water Conservation*, 31(2): 97–102. (in Chinese)
- Hu Y h, Gao M, Batunacun, 2020. Evaluations of water yield and soil erosion in the Shaanxi-Gansu Loess Plateau under different land use and climate change scenarios. *Environmental Development*, 34: 100488. doi: 10.1016/j.envdev.2019.100488
- Huang Zhihua, Zhao Jun, Xiao Hanyu et al., 2021. Water service supply and demand situation and driving factors in Shiyang River Basin. *Journal of Soil and Water Conservation*, 35(3): 228–235. (in Chinese)
- Jiang Taiming, Wei Chaofu, Xie Deti et al., 2006. Study on water holding capacity of yellow soil in karst area of central Guizhou. *Journal of Soil and Water Conservation*, 20(6): 25–29. (in Chinese)
- Jiang Z C, Lian Y Q, Qin X Q, 2014. Rocky desertification in Southwest China: impacts, causes, and restoration. *Earth-Science Reviews*, 132: 1–12. doi: 10.1016/j.earscirev.2014.01.005
- Kovacs K, Polasky S, Nelson E et al., 2013. Evaluating the return in ecosystem services from investment in public land acquisitions. *PloS one*, 8(6): e62202. doi: 10.1371/journal.pone.0062202
- Kuang Xueyuan, Su Zhi, Tu Fangxu, 2007. Climate regionalization of Guangxi. *Guangxi Science*, 14(3): 278–283. (in Chinese)
- Lang Y Q, Song W, Zhang Y, 2017. Responses of the water-yield ecosystem service to climate and land use change in Sancha River Basin, China. *Physics and Chemistry of the Earth, Parts A/B/C*, 101: 102–111. doi: 10.1016/j.pce.2017.06.003
- Lang Y Q, Song W, 2018. Trade-off analysis of ecosystem services in a mountainous Karst Area, China. *Water*, 10(3): 300. doi: 10.3390/w10030300
- Li G Y, Jiang C H, Zhang Y H et al., 2021. Whether land greening in different geomorphic units are beneficial to water yield in the Yellow River Basin? *Ecological Indicators*, 120: 106926. doi: 10.1016/j.ecolind.2020.106926
- Li Li, Zhao Fang, Zhu Lianqi et al., 2021. Geographical detection of ecosystem services trade-offs and their spatial variation mechanism in Qihe River Basin. *Acta Ecologica Sinica*, 41(19): 7568–7578. (in Chinese)
- Li M Y, Liang D, Xia J et al., 2021c. Evaluation of water conservation function of Danjiang River Basin in Qinling Mountains, China based on InVEST model. *Journal of Environmental Management*, 286: 112212. doi: 10.1016/j.jenvman.2021.112212
- Li Shuai, Deng Wanzhen, Li Jian et al., 2021d. Effect of tillage on soil moisture and rainfall response mechanism in karst areas of Guangxi. *Water Saving Irrigation*, (6): 31–36. (in Chinese)
- Lian X H, Qi Y, Wang H W et al., 2019. Assessing changes of water yield in qinghai lake watershed of China. *Water*, 12(1): 11. doi: 10.3390/w12010011
- Liang L Q, Liu Q, 2014. Streamflow sensitivity analysis to climate change for a large water-limited basin. *Hydrological Processes*, 28(4): 1767–1774. doi: 10.1002/hyp.9720
- Luo Guangjie, 2016. Extraction information and development strategy of ecological optimizing for small karst watersheds Beijing: University of Chinese Academy of Sciences. (in Chinese)
- Marquès M, Bangash R F, Kumar V et al., 2013. The impact of climate change on water provision under a low flow regime: a case study of the ecosystems services in the Francoli river basin. *Journal of Hazardous Materials*, 263: 224–232. doi: 10.1016/j.jhazmat.2013.07.049
- Pan Lizhong, Jin Maogao, 1996. Comparison of water resources statistical indicators between China and other countries. *Advances in Water Science*, 7(4): 375–380. (in Chinese)
- Pei H W, Liu M Z, Shen Y J et al., 2021. Quantifying impacts of climate dynamics and land-use changes on water yield service in the agro-pastoral ecotone of northern China. *Science of the Total Environment*, 809: 151153. doi: 10.1016/j.scitotenv.2021.151153
- Qi X K, Li Q, Yue Y M et al., 2021. Rural-urban migration and conservation drive the ecosystem services improvement in China Karst: a case study of Huanjiang County, Guangxi. *Remote Sensing*, 13(4): 566. doi: 10.3390/rs13040566
- Sánchez-Canales M, Benito A L, Passuello A et al., 2012. Sensitivity analysis of ecosystem service valuation in a Mediterranean watershed. *Science of the Total Environment*, 440: 140–153. doi: 10.1016/j.scitotenv.2012.07.071
- Sharp R, Tallis H T, Ricketts T et al., 2014. *InVEST User's Guide*. In: The Natural Capital Project. CA, USA: Stanford.
- Stevanović Z, 2019. Karst waters in potable water supply: a global scale overview. *Environmental Earth Sciences*, 78(23): 622. doi: 10.1007/s12665-019-8670-9
- Wada Y, Beek L P H, Kempen C M et al., 2010. Global depletion of groundwater resources. *Geophysical Research Letters*, 37(20): L20402. doi: 10.1029/2010gl044571
- Wan H W, Li H X, Wu J H et al., 2021. Spatial distribution pattern in mammal and bird richness and their relationship with ecosystem services in Sanjiangyuan National Park, China. *Journal of Mountain Science*, 18(6): 1662–1677. doi: 10.1007/

- s11629-020-6515-3
- Wang Baosheng, Chen Huaxiang, Dong Zheng et al., 2020. Impact of land use change on the water conservation service of ecosystems in the urban agglomeration of the Golden Triangle of Southern Fujian, China, in 2030. *Acta Ecologica Sinica*, 40(2): 484–498. (in Chinese)
- Wang H, Liu L B, Yin L et al., 2021. Exploring the complex relationships and drivers of ecosystem services across different geomorphological types in the Beijing-Tianjin-Hebei region, China (2000–2018). *Ecological Indicators*, 121: 107116. doi: [10.1016/j.ecolind.2020.107116](https://doi.org/10.1016/j.ecolind.2020.107116)
- Wang Jinfeng, Xu Chengdong, 2017. Geodetector: principle and prospective. *Acta Geographica Sinica*, 72(1): 116–134. (in Chinese)
- Wang Shijie, Zhang Xinbao, Bai Xiaoyong, 2013. Discussion on nomenclature of the karst desertification regions and illustration for their environment characteristics in Southwest China. *Mountain Research*, 31(1): 18–24. (in Chinese)
- Wang T H, Song H Q, Wang F et al., 2020. Hysteretic effects of meteorological conditions and their interactions on particulate matter in Chinese cities. *Journal of Cleaner Production*, 274: 122926. doi: [10.1016/j.jclepro.2020.122926](https://doi.org/10.1016/j.jclepro.2020.122926)
- Wang X, Chu B, Feng X et al., 2021. Spatiotemporal variation and driving factors of water yield services on the Qingzang Plateau. *Geography and Sustainability*, 2(1): 31–39. doi: [10.1016/j.geosus.2021.02.002](https://doi.org/10.1016/j.geosus.2021.02.002)
- Wang Xiaofeng, Zhang Xinrong, Feng Xiaoming et al., 2020. Trade-offs and synergies of ecosystem services in karst area of China driven by Grain-for-Green Program. *Chinese Geographical Science*, 30(1): 101–114. doi: [10.1007/s11769-020-1098-z](https://doi.org/10.1007/s11769-020-1098-z)
- Wang Xiuming, Liu Xucheng, Long Yingxian et al., 2020. Spatial-temporal changes and influencing factors of ecosystem services in Shaoguan City based on improved InVEST. *Research of Soil and Water Conservation*, 27(5): 380–388. (in Chinese)
- Wang Yahui, Dai Erfu, Ma Liang et al., 2020e. Spatiotemporal and influencing factors analysis of water yield in the Hengduan Mountain region. *Journal of Natural Resources*, 35(2): 371–386. (in Chinese). doi: [10.31497/zrzyxb.20200210](https://doi.org/10.31497/zrzyxb.20200210)
- Wang Ying, Su Yongxiu, Li Zheng, 2013. Responses of temperature change in Guangxi to global warming during 1961–2010. *Journal of Natural Resources*, 28(10): 1707–1717. (in Chinese)
- Wang Yuchun, Zhao Jun, Fu Jiewen et al., 2018. Quantitative assessment of water conservation function and spatial pattern in Shiyang River Basin. *Acta Ecologica Sinica*, 38(13): 4637–4648. (in Chinese)
- Wei P J, Chen S Y, Wu M H et al., 2021. Using the InVEST model to assess the impacts of climate and land use changes on water yield in the upstream regions of the Shule River Basin. *Water*, 13(9): 1250. doi: [10.3390/w13091250](https://doi.org/10.3390/w13091250)
- Wu Xiebao, Sun Jilin, Lin Qiong et al., 2009. Research on division treatment to eco-construction of karst rock deserted land in southwest China karst area. *Carsologica Sinica*, 28(4): 391–396. (in Chinese)
- Wu Zhe, Chen Xin, Liu Beibei et al., 2013. Risk assessment of nitrogen and phosphorus loads in Hainan Island based on InVEST model. *Chinese Journal of Tropical Crops*, 34(9): 1791–1797. (in Chinese)
- Xia Lin, An Yulun, Jiang Haifeng et al., 2019. Water conservation of karst river basins based on InVEST model: a case study of Wujiang River Basin in Guizhou. *Guizhou Science*, 37(1): 27–32. (in Chinese)
- Xiao Yang, Ouyang ZhiYun, 2019. Spatial-temporal patterns and driving forces of water retention service in China. *Chinese Geographical Science*, 29(1): 100–111. doi: [10.1007/s11769-018-0984-0](https://doi.org/10.1007/s11769-018-0984-0)
- Xiong Pingsheng, Yuan Daoxian, Xie Shiyong, 2010. Progress of research on rocky desertification in south China karst mountain. *Carsologica Sinica*, 29(4): 355–362. (in Chinese)
- Xu X L, Liu W, Scanlon B R et al., 2013. Local and global factors controlling water-energy balances within the Budyko framework. *Geophysical Research Letters*, 40(23): 6123–6129. doi: [10.1002/2013GL058324](https://doi.org/10.1002/2013GL058324)
- Yang Jie, Xie Baopeng, Zhang Degang, 2020. Spatio-temporal variation of water yield and its response to precipitation and land use change in the Yellow River Basin based on InVEST model. *Chinese Journal of Applied Ecology*, 31(8): 2731–2739. (in Chinese)
- Yang Xianwu, 2019. DEM based research on the topographic characteristics and spatial variation of Fenglin and Fengcong karst landforms. Nanjing: Nanjing Normal University. (in Chinese)
- Zhang Dianfa, Ouyang Ziyuan, Wang Shijie, 2001. Population resources environment and sustainable development in the karst region of southwest China. *China Population, Resources and Environment*, 11(1): 77–81. (in Chinese)
- Zhang Ze, Hu Baoqing, Qiu Haihong et al., 2021. Spatio-temporal differentiation and driving mechanism of ecological environment vulnerability in Southwest Guangxi Karst-Beibu gulf coastal zone. *Journal of Geo-information Science*, 23(3): 456–466. (in Chinese)
- Zheng Jingyun, Yin Yunhe, Li Bingyuan, 2010. A new scheme for climate regionalization in China. *Acta Geographica Sinica*, 65(1): 3–12. (in Chinese)
- Zheng Xu, Wei Lemin, Guo Jianjun et al., 2020. Driving force analysis of water yield in inland river basins of arid areas based on Geo-detectors: a case of the Shule River. *Arid Land Geography*, 43(6): 1477–1485. (in Chinese)
- Zhu Dehao, 1982. Evolution of peak cluster-depression in Guilin area and morphometric measurement. *Carsologica Sinica*, (2): 127–134. (in Chinese)
- Zuo L Y, Gao J B, Du F J, 2021. The pairwise interaction of environmental factors for ecosystem services relationships in karst ecological priority protection and key restoration areas. *Ecological Indicators*, 131: 108125. doi: [10.1016/j.ecolind.2021.108125](https://doi.org/10.1016/j.ecolind.2021.108125)